$P\bar{6}m2$, $P6_3mc$, $P6_3/mmc$, $R3m$, $R\bar{3}m$, and $Fm3m$. The last space group corresponds to the special case of cubic close packing $/ABC/\ldots$. The tetrahedral arrangement of Si and C in SiC does not permit either a centre of symmetry ($\bar{1}$) or a plane of symmetry (m) perpendicular to [00.1]. SiC structures can therefore have only four possible space groups $P3m1$, $R3m1$, $P6_3mc$, and $F\bar{4}3m$. CdI_2 structures can have a centre of symmetry on octahedral voids, but cannot have a symmetry plane perpendicular to [00.1]. CdI_2 can therefore have five possible space groups: $P3m1$, $P\bar{3}m$, $R3m$, $R\bar{3}m$, and $P6_3mc$. Cubic symmetry is not possible in CdI_2 on account of the presence of Cd atoms, the sequence $/A\gamma BC\beta AB\alpha C/$ representing a 6R structure.

9.2.1.6. *Crystallographic uses of Zhdanov symbols*

From the Zhdanov symbols of a close-packed structure, it is possible to derive information about the symmetry and lattice type (Verma & Krishna, 1966). Let n_+ and n_- be the number of positive and negative numerals in the Zhdanov sequence of a given structure. The lattice is rhombohedral if $n_+ - n_- = \pm 1 \bmod 3$, otherwise it is hexagonal. The + sign corresponds to the reverse setting and − to the obverse setting of the rhombohedral lattice. Since this criterion is sufficient for the identification of a rhombohedral structure, the practice of writing three units of identical Zhdanov symbols has been abandoned in recent years (Pandey & Krishna, 1982*a*). Thus the 15R polytype of SiC is written as (23) rather than $(23)_3$.

As described in detail by Verma & Krishna (1966), if the Zhdanov symbol consists of an odd set of numbers repeated twice, *e.g.* (22), (33), (221221) *etc.*, the structure can be shown to possess a 6_3 axis. For the centre of symmetry at the centre of a sphere or an octahedral void, the Zhdanov symbol will consist of a symmetrical arrangement of numbers of like signs surrounding a single even or odd Zhdanov number, respectively. Thus, the structures (2)32(4)23 and (3)32(5)23 have centres of symmetry of the two types in the numbers within parentheses. For structures with a symmetry plane perpendicular to [00.1], the Zhdanov symbols consist of a symmetrical arrangement of a set of numbers of opposite signs about the space between two succession numbers. Thus, a stacking |522|225| has mirror planes at positions indicated by the vertical lines.

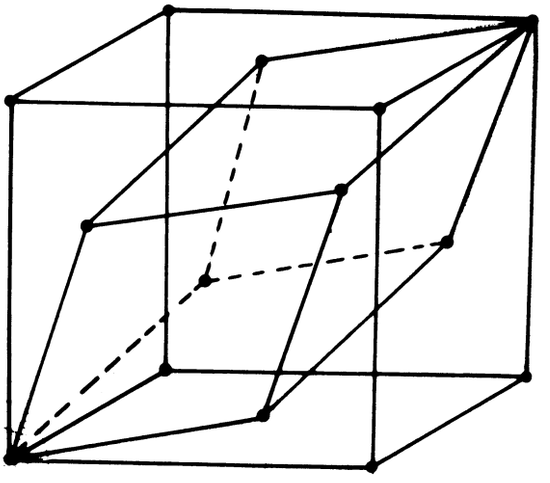

Fig. 9.2.1.8. The relationship between the f.c.c. and the primitive rhombohedral unit cell of the c.c.p. structure.

The use of abridged symbols to describe crystal structures has sometimes led to confusion in deciding the crystallographic equivalence of two polytype structures. For example, the structures (13) and (31) are identical for SiC but not for CdI_2 (Jain & Trigunayat, 1977*a*,*b*).

9.2.1.7. *Structure determination of close-packed layer stackings*

9.2.1.7.1. *General considerations*

The different layer stackings (polytypes) of the same material have identical a and b parameters of the direct lattice. The a^*b^* reciprocal-lattice net is therefore also the same and is shown in Fig. 9.2.1.9. The reciprocal lattices of these polytypes differ only along the c^* axis, which is perpendicular to the layers. It is evident from Fig. 9.2.1.9 that for each reciprocal-lattice row parallel to $\mathbf{c}^*$ there are five others with the same value of the radial coordinate ξ. For example, the rows 10.l, 01.l, $\bar{1}1.l$, $\bar{1}0.l$, $0\bar{1}.l$, and $1\bar{1}.l$ all have $\xi = |\mathbf{a}^*|$. Owing to symmetry considerations, it is sufficient to record any one of them on X-ray diffraction photographs. The reciprocal-lattice rows $hk.l$ can be classified into two categories according as $h - k = 0 \bmod 3$ or $\pm 1 \bmod 3$. Since the atoms in an nH or nR structure lie on three symmetry axes $A : [00.1]_{00}$, $B : [00.1]_{\frac{1}{3},-\frac{1}{3}}$, and $C : [00.1]_{-\frac{1}{3},\frac{1}{3}}$, the structure factor F_{hkl} can be split into three parts:

$$F_{hkl} = P + Q\exp[2\pi i(h-k)/3] + R\exp[-2\pi i(h-k)/3],$$

where $P = \sum_{z_A} \exp(2\pi i l z_A/n)$, $Q = \sum_{z_B} \exp(2\pi i l z_B/n)$, $R = \sum_{z_C} \exp(2\pi i l z_C/n)$, and z_A/n, z_B/n, z_C/n are the z coordinates of atoms at A, B, and C sites, respectively. For $h - k = 0 \bmod 3$,

$$F_{hkl} = P + Q + R = \sum_{z=0}^{n=-1} \exp(2\pi i l z/n),$$

which is zero except when $l = 0, n, 2n, \ldots$. Hence, the reflections 00.l, 11.l, 30.l, *etc.*, for which $h - k = 0 \bmod 3$, will be extinguished except when $l = 0, n, 2n, \ldots$. Thus, only those $hk.l$ reciprocal-lattice rows for which $h - k \neq 0 \bmod 3$ carry information about the stacking sequence and contain in general reflections with $l = 0, 1, 2, \ldots, n-1$, *etc.* It is sufficient to record any one such row, usually the 10.l row with $\xi = |\mathbf{a}^*|$, on an oscillation, Weissenberg, or precession photograph to obtain information about the lattice type, identity period, space group, and hence the complete structure (Verma & Krishna, 1966).

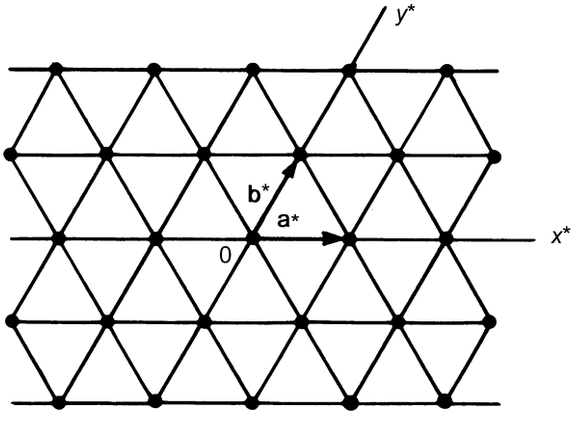

Fig. 9.2.1.9. The $\mathbf{a}^*$–$\mathbf{b}^*$ reciprocal-lattice net for close-packed layer stackings.

9.2.1.7.2. *Determination of the lattice type*

When the structure has a hexagonal lattice, the positions of spots are symmetrical about the zero layer line on the *c*-axis oscillation photograph. However, the intensities of the reflections on the two sides of the zero layer line are the same only if the structure possesses a 6_3 axis, and not for the trigonal system. An apparent mirror symmetry perpendicular to the *c* axis results from the combination of the 6_3 axis with the centre of symmetry introduced by X-ray diffraction. For a structure with a rhombohedral lattice, the positions of X-ray diffraction spots are not symmetrical about the zero layer line because the hexagonal unit cell is non-primitive causing the reflections *hkl* to be absent when $-h + k + l \neq 3n$ ($\pm n = 0, 1, 2, \ldots$). For the 10.*l* row, this means that the permitted reflections will have $l = 3n + 1$, which implies above the zero layer line $10.\bar{1}$, $10.\bar{4}$, $10.\bar{7}$, *etc*. reflections and below the zero layer line $10.\bar{2}$, $10.\bar{5}$, $10.\bar{8}$, *etc*. The zero layer line will therefore divide the distance between the nearest spots on either side (namely 10.1 and $10.\bar{2}$) approximately in the ratio 1:2. This enables a quick identification of a rhombohedral lattice. It is also possible to identify rhombohedral lattices by the appearance of an apparent 'doubling' of spots along the Bernal row lines on a rotation photograph. This is because of the threefold symmetry which makes reciprocal-lattice rows such as 10.*l*, $\bar{1}1.l$, and $01.\bar{l}$ identical with each other but different from the other identical set, 01.*l*, $\bar{1}0.l$, and $1\bar{1}.l$. The extinction condition for the second set requires $l = 3n - 1$, *i.e.* $l = 2, 5, 8$, and $\bar{1}, \bar{4}, \bar{7}$, *etc.*, which is different from that for the first set. Consequently, on the rotation photograph, reciprocal-lattice rows with $\xi = |\mathbf{a}^*|$ will have spots for $l = 3n \pm 1$ causing the apparent 'doubling'.

In crystals of layer structures, such as CdI_2, where *a*-axis oscillation photographs are normally taken, the identification of the rhombohedral lattice is performed by checking for the non-coincidence of the diffraction spots with those for the 2*H* or 4*H* structures. In an alternative method, one compares the positions of spots in two rows of the type 10.*l* and 20.*l*. This can conveniently be done by taking a Weissenberg photograph (Chadha, 1977).

9.2.1.7.3. *Determination of the identity period*

The number of layers, *n*, in the hexagonal unit cell can be found by determining the *c* parameter from the *c*-axis rotation or oscillation photographs and dividing this by the layer spacing *h* for that compound which can be found from reflections with $h - k = 0 \bmod 3$. The density of reciprocal-lattice points along rows parallel to $\mathbf{c}^*$ depends on the periodicity along the *c* axis. The larger the identity period along **c**, the more closely spaced are the diffraction spots along $\mathbf{c}^*$. In situations where there are not many structural extinctions, *n* can be determined by counting the number of spacings after which the sequence of relative intensities begins to repeat along the 10.*l* row of spots on an oscillation or Weissenberg photograph (Krishna & Verma, 1963). If the structure contains a random stacking disorder of close-packed layers (stacking faults), this will effectively make the **c** parameter infinite ($\mathbf{c}^* \rightarrow 0$) and lead to the production of characteristic continuous diffuse streaks along reciprocal-lattice rows parallel to $\mathbf{c}^*$ for reflections with $h - k \neq 0 \bmod 3$ (Wilson, 1942). It is therefore difficult to distinguish by X-ray diffraction between structures of very large unresolvable periodicities and those with random stacking faults. Lattice resolution in the electron microscope has been used in recent years to identify such structures (Dubey, Singh & Van Tendeloo, 1977). A better resolution of diffraction spots along the 10.*l* reciprocal-lattice row can be obtained by using the Laue method. Standard charts for rapid identification of SiC polytypes from Laue films are available in the literature (Mitchell, 1953). Identity periods as large as 594 layers have been resolved by this method (Honjo, Miyake & Tomita, 1950). Synchrotron radiation has been used for taking Laue photographs of ZnS polytypes (Steinberger, Bordas & Kalman, 1977).

9.2.1.7.4. *Determination of the stacking sequence of layers*

For an *nH* or 3*nR* polytype, the *n* close-packed layers in the unit cell can be stacked in 2^{n-1} possible ways, all of which cannot be considered for ultimate intensity calculations. A variety of considerations has therefore been used for restricting the number of trial structures. To begin with, symmetry and space-group considerations discussed in Subsection 9.2.1.4 and 9.2.1.5 can considerably reduce the number of trial structures.

When the short-period structures act as 'basic structures' for the generation of long-period polytypes, the number of trial structures is considerably reduced since the crystallographic unit cells of the latter will contain several units of the small-period structures with faults between or at the end of such units. The basic structure of an unknown polytype can be guessed by noting the intensities of 10.*l* reflections that are maximum near the positions corresponding to the basic structure. If the unknown polytype belongs to a well known structure series, such as $(33)_n32$ and $(33)_n34$ based on SiC-6*H*, empirical rules framed by Mitchell (1953) and Krishna & Verma (1962) can allow the direct identification of the layer-stacking sequence without elaborate intensity calculations.

It is possible to restrict the number of probable structures for an unknown polytype on the basis of the faulted matrix model of polytypism for the origin of polytype structures (for details see Pandey & Krishna, 1983). The most probable series of structures as predicted on the basis of this model for SiC contains the numbers 2, 3, 4, 5 and 6 in their Zhdanov sequence (Pandey & Krishna, 1975, 1976*a*). For CdI_2 and PbI_2 polytypes, the possible Zhdanov numbers are 1, 2 and 3 (Pandey & Krishna, 1983; Pandey, 1985). On the basis of the faulted matrix model, it is not only possible to restrict the numbers occurring in the Zhdanov sequence but also to restrict drastically the number of trial structures for a new polytype.

Structure determination of ZnS polytypes is more difficult since they are not based on any simple polytype and any number can appear in the Zhadanov sequence. It has been observed that the birefringence of polytype structures in ZnS varies linearly with the percentage hexagonality (Brafman & Steinberger, 1966), which in turn is related to the number of reversals in the stacking sequence, *i.e.* the number of numbers in the Zhdanov sequence. This drastically reduces the number of trial structures for ZnS (Brafman, Alexander & Steinberger, 1967).

Singh and his co-workers have successfully used lattice imaging in conjunction with X-ray diffraction for determining the structures of long-period polytypes of SiC that are not based on a simple basic structure. After recording X-ray diffraction patterns, single crystals of these polytypes were crushed to yield electron-beam-transparent flakes. The one- and two-dimensional lattice images were used to propose the possible structures for the polytypes. Usually this approach leads to a very few possibilities and the correct structure is easily determined by comparing the observed and calculated X-ray intensities for the proposed structures (Dubey & Singh, 1978; Rai, Singh, Dubey & Singh, 1986).

Direct methods for the structure determination of polytypes from X-ray data have also been suggested by several workers (Tokonami & Hosoya, 1965; Dornberger-Schiff & Farkas-

Jahnke, 1970; Farkas-Jahnke & Dornberger-Schiff, 1969) and have been reviewed by Farkas-Jahnke (1983). These have been used to derive the structures of ZnS, SiC, and $TiS_{1.7}$ polytypes. These methods are extremely sensitive to experimental errors in the intensities.

9.2.1.8. *Stacking faults in close-packed structures*

The two alternative positions for the stacking of successive close-packed layers give rise to the possibility of occurrence of faults where the stacking rule is broken without violating the law of close packing. Such faults are frequently observed in crystals of polytypic materials as well as close-packed martensites of cobalt, noble-metal-based and certain iron-based alloys (Andrade, Chandrasekaran & Delaey 1984; Kabra, Pandey & Lele, 1988*a*; Nishiyama, 1978; Pandey, 1988).

The classical method of classifying stacking faults in 2*H* and 3*C* structures as growth and deformation types, depending on whether the fault has resulted as an accident during growth or by shear through the vector **s**, leads to considerable ambiguities since the same fault configuration can result from more than one physical process. For a detailed account of the limitations of the notations based on the process of formation, the reader is referred to the articles by Pandey (1984*a*) and Pandey & Krishna (1982*b*).

Frank (1951) has classified stacking faults as intrinsic or extrinsic purely on geometrical considerations. In intrinsic faults, the perfect stacking sequence on each side of the fault extends right up to the contact plane of the two crystal halves while in extrinsic faults the contact plane does not belong to the stacking sequence on either side of it. In intrinsic faults, the contact plane may be an atomic or non-atomic plane whereas in extrinsic faults the contact plane is always an atomic plane. Instead of contact plane, one can use the concept of fault plane defined with respect to the initial stacking sequence. This system of classification is preferable to that based on the process of formation. However, the terms intrinsic and extrinsic have been used in the literature in a very restricted sense by associating these with the precipitation of vacancies and interstitials, respectively (see, for example, Weertman & Weertman, 1984). While the precipitation of vacancies may lead to intrinsic fault configuration, this is by no means the only process by which intrinsic faults can result. For example, there are geometrically 18 possible intrinsic fault configurations in the 6*H* (33) structure (Pandey & Krishna, 1975) but only two of these can result from the precipitation of vacancies. Similarly, layer-displacement faults involved in SiC transformations are extrinsic type but do not result from the precipitation of interstitials (see Pandey, Lele & Krishna, 1980*a*,*b*,*c*; Kabra, Pandey & Lele, 1986). It is therefore desirable not to associate the geometrical notation of Frank with any particular process of formation.

The intrinsic–extrinsic scheme of classification of faults when used in conjunction with the concept of assigning subscripts to different close-packed layers (Prasad & Lele, 1971; Pandey & Krishna, 1976*b*) can provide a very compact and unique way of representing intrinsic fault configurations even in long-period structures (Pandey, 1984*b*). We shall briefly explain this notation in relation to one hexagonal (6*H*) and one rhombohedral (9*R*) structure.

In the 6*H* (*ABCACB*, ... or *hkkhkk*) structure, six kinds of layers that can be assigned subscripts 0, 1, 2, 3, 4, and 5 need to be distinguished (Pandey, 1984*b*). Choosing the 0-type layer in '*h*' configuration such that the layer next to it is related through the shift vector $+\mathbf{s}$ (which causes cyclic $A \rightarrow B \rightarrow C \rightarrow A$ shift), the perfect 6*H* structure can be written as

$$\begin{array}{cccccccccccc} & h & k & k & h & k & k & h & k & k & h & k & k & \\ \ldots & A_0 & B_1 & C_2 & A_3 & C_4 & B_5 & A_0 & B_1 & C_2 & A_3 & C_4 & B_5 & \ldots. \\ & +\mathbf{s} & +\mathbf{s} & +\mathbf{s} & -\mathbf{s} & -\mathbf{s} & -\mathbf{s} & +\mathbf{s} & +\mathbf{s} & +\mathbf{s} & -\mathbf{s} & -\mathbf{s} & & \end{array}$$

There are six crystallographically equivalent ways of writing this structure with the first layer in position *A*: (i) $A_0B_1C_2A_3C_4B_5$; (ii) $A_1B_2C_3B_4A_5C_0$; (iii) $A_2B_3A_4C_5B_0C_1$; (iv) $A_3C_4B_5A_0B_1C_2$; (v) $A_4C_5B_0C_1A_2B_3$; and (vi) $A_5C_0A_1B_2C_3B_4$. Similarly, there are six ways of writing the 6*H* structure with the starting layer in position *B* or *C*. Since an intrinsic fault marks the beginning of a fresh 6*H* sequence, there can be 36 possible intrinsic fault configurations in the 6*H* (*ABCACB*, ...) structure. All these intrinsic fault configurations can be described by symbols like $I_{r,s}$, where *r* and *s* stand for the subscript of the layer on the left- and right-hand sides of the fault plane while *I* represents intrinsic. Knowing the two symbols (*r* and *s*), one can write down the complete *ABC* stacking sequence. It may be noted that, of the 36 possible intrinsic fault configurations, only 14 are crystallographically indistinguishable (for details, see Pandey, 1984*b*). This notation can be used for any hexagonal polytype and requires only the identification of various layer types in the structure. For rhombohedral polytypes, one must consider the layer types in both the obverse and the reverse settings. For example, six layer types need to be distinguished in the 9*R* (*hhk*) structure:

Obverse:

$$\begin{array}{cccccccccc} & h & h & k & h & h & k & h & h & k & \\ \ldots & A_0 & B_1 & A_2 & C_0 & A_1 & C_2 & B_0 & C_1 & B_2 & \ldots; \\ & +\mathbf{s} & -\mathbf{s} & -\mathbf{s} & +\mathbf{s} & -\mathbf{s} & -\mathbf{s} & +\mathbf{s} & -\mathbf{s} & & \end{array}$$

Table 9.2.1.3. *Intrinsic fault configurations in the 6H* $(A_0B_1C_2A_3C_4B_5, \ldots)$ *structure*

Fault configuration *ABC* sequence	Subscript notation
$\ldots A\ B\ C\ A\ C\ B\ A_0 \mid C_0\ A\ B\ C\ B\ A\ C \ldots$	$I_{0,0}$
$\ldots A\ B\ C\ A\ C\ B\ A_0 \mid C_1\ A\ B\ A\ C\ B\ C \ldots$	$I_{0,1}$
$\ldots A\ B\ C\ A\ C\ B\ A_0 \mid C_2\ A\ C\ B\ A\ B\ C \ldots$	$I_{0,2}$
$\ldots A\ B\ C\ A\ C\ B\ A_0 \mid C_3\ B\ A\ C\ A\ B\ C \ldots$	$I_{0,3}$
$\ldots A\ B\ C\ A\ C\ B\ A_0 \mid C_4\ B\ A\ B\ C\ A\ C \ldots$	$I_{0,4}$
$\ldots A\ B\ C\ A\ C\ B\ A_0 \mid C_5\ B\ C\ A\ B\ A\ C \ldots$	$I_{0,5}$
$\ldots A\ B\ C\ A\ C\ B\ A\ B_1 \mid A_0\ B\ C\ A\ C\ B\ A \ldots$	$I_{1,0}$
$\ldots A\ B\ C\ A\ C\ B\ A\ B_1 \mid A_1\ B\ C\ B\ A\ C\ A \ldots$	$I_{1,1}$
$\ldots A\ B\ C\ A\ C\ B\ A\ B_1 \mid A_2\ B\ A\ C\ B\ C\ A \ldots$	$I_{1,2}$
$\ldots A\ B\ C\ A\ C\ B\ A\ B_1 \mid A_3\ C\ B\ A\ B\ C\ A \ldots$	$I_{1,3}$
$\ldots A\ B\ C\ A\ C\ B\ A\ B_1 \mid A_4\ C\ B\ C\ A\ B\ A \ldots$	$I_{1,4}$
$\ldots A\ B\ C\ A\ C\ B\ A\ B_1 \mid A_5\ C\ A\ B\ C\ B\ A \ldots$	$I_{1,5}$
$\ldots A\ B\ C\ A\ C\ B\ A\ B\ C_2 \mid B_0\ C\ A\ B\ A\ C\ B \ldots$	$I_{2,0}$
$\ldots A\ B\ C\ A\ C\ B\ A\ B\ C_2 \mid B_1\ C\ A\ C\ B\ A\ B \ldots$	$I_{2,1}$
$\ldots A\ B\ C\ A\ C\ B\ A\ B\ C_2 \mid B_2\ C\ B\ A\ C\ A\ B \ldots$	$I_{2,2}$
$\ldots A\ B\ C\ A\ C\ B\ A\ B\ C_2 \mid B_3\ A\ C\ B\ C\ A\ B \ldots$	$I_{2,3}$
$\ldots A\ B\ C\ A\ C\ B\ A\ B\ C_2 \mid B_4\ A\ C\ A\ B\ C\ B \ldots$	$I_{2,4}$
$\ldots A\ B\ C\ A\ C\ B\ A\ B\ C_2 \mid B_5\ A\ B\ C\ A\ C\ B \ldots$	$I_{2,5}$

Notes:

(1) Dotted vertical lines represent the location of the fault plane with respect to the initial stacking sequence on the left-hand side.

(2) $I_{0,1}$ and $I_{2,3}$, $I_{0,2}$ and $I_{1,3}$, $I_{1,1}$ and $I_{2,2}$, and $I_{1,4}$ and $I_{2,5}$ are crystallographically equivalent.